MEMBRANE DIFFERENTIATIONS IN FREEZE-FRACTURED MAMMALIAN SPERM

DANIEL S. FRIEND and DON W. FAWCETT

With the technical assistance of IRENE RUDOLF

From the Department of Pathology, University of California, San Francisco, California 94143 and the Department of Anatomy, Harvard Medical School, Boston, Massachusetts 02115

ABSTRACT

A correlated thin-sectioning and freeze-fracturing study has been made of guinea pig and rat spermatozoa. In sections, the cell membrane over the acrosome has a concanavalin A and ruthenium red reactive glycocalyx which exhibits an ordered pattern related to the lattice of crystalline domains within the plane of the membrane revealed by freeze-fracturing. The cleaved acrosomal membrane also shows a finer linear periodicity in some areas.

The membrane over the equatorial segment of the guinea pig acrosome is marked by a palisade of oblique ridges not observed in the rat. The plasmalemma of the postacrosomal region is rich in membrane intercalated particles, many randomly dispersed, others clustered in rectilinear arrays. A particle-poor zone is found just anterior to the posterior ring. The fold of redundant nuclear envelope posterior to the ring has many nuclear pores in close hexagonal array. The nuclear envelope lining the implantation fossa is devoid of pores. When cleaved it has a particle-free central area surrounded by a broad zone of large, closely packed, hollow particles.

The membrane of the mid-piece in the guinea pig (but not the rat) contains linear strands of 6–8-nm particles oriented circumferentially. The membrane investing the principal piece exhibits the usual randomly distributed particles but in addition, a double row of larger (9 nm) particles runs longitudinally within the membrane over outer dense fiber 1. In the corresponding position in thin sections a local thickening of the membrane is discernible. These observations form a basis for further studies on the functional correlates of these regional specializations of the sperm membrane.

Considerable specificity exists in the interaction of sperm and egg in mammalian fertilization, a specificity which favors the recognition and attachment of gametes of the same species and discourages hybridization. Apparently this specificity resides in the membranes. In addition, there is a remarkable regional specialization of the sperm surface. Only the membrane overlying the acrosome is involved in the normal adhesion of epididymal sperm in the guinea pig and opossum (8), in the adhesion of sperm to leukocytes (unpublished observations), and in the head-to-head sperm agglutination in the presence of certain antisera (33). It is this membrane region,

too, which specializes in participating in the acrosome reaction (1–4, 9). In contrast, the postacrosomal region is the portion of the sperm membrane that coalesces with the oolemma in fertilization (46, 47). The membrane overlying the midpiece is presumably concerned with the access of substrate to the energy-generating mechanism of the underlying mitochondrial sheath, while the membrane of the principal piece, unusually permeable (10), evidently has properties permitting numerous deformations associated with the propagation of bending waves along the flagellum. In view of these functional differences, we would expect to find corresponding differences in the several regions of the cell membrane. Histochemical evidence of regional differences in surface charge has been reported (3, 4, 45, 48), and the distribution of certain oligosaccharides on the sperm surface has been mapped with concanavalin A and other lectin probes (11, 36).

Freeze-fracturing, followed by examination of high-fidelity replicas of the frozen surfaces, affords a more direct visual examination of structural specializations within the plane of the membrane (6). To date, however, this approach has been relatively unexploited by biologists concerned with reproduction. But in several species, the freeze-fracturing of sperm has revealed multiple intramembranous particles in the plasma membrane, sometimes in ordered arrays (17, 18–20, 25–29, 37, 40). Mindful of Branton's and Deamer's observation that membranes rich in biological activity are generally also particle-rich in freeze-fractured preparations (6), we would expect to find elaborate arrays of particles in some of the deeper-lying membranes of the sperm head as well as in various regions of the plasmalemma. For example, the inner acrosomal membrane is believed to be rich in trypsin-like protease, enabling sperm to penetrate the zona pellucida (22, 42).

We have here described in detail the corresponding thin-section and freeze-fracture appearance of membranes from intact guinea pig and rat sperm removed from the posterior segment of the epididymis. In a subsequent paper, we will describe the alterations which occur after in vitro induction of acrosomal disruption, that is, destruction of the plasma membrane and outer acrosomal membrane when sperm is mixed with the fallopian tubal contents of superovulated female rodents.

MATERIALS AND METHODS

Materials

The tissues and organs used in these studies were the testes, epididymides, vasa deferentia, and sperm removed from the latter two structures of sexually mature Sprague-Dawley rats and guinea pigs. Approximately 8 guinea pigs and 12 rats, plus the following reagents, were employed: concanavalin A, ruthenium red, 3,3'-diaminobenzidine tetrahydrochloride (Sigma Chemical Co., St. Louis, Mo.); horseradish peroxidase (Worthington Biochemical Corp., Freehold, N. J.); K ferrocyanide (Fisher Scientific Company, Springfield, N. J.); tissue culture medium RPMI 1640 with added glutamine (Grand Island Biological Co., Oakland, Calif.); and tannic acid (Merck and Co., Inc., Rahway, N. J.).

Methods

PREPARATION OF THIN SECTIONS: Fixation of tissues *in situ* was initiated by local injection of 1–2 ml fixative containing 1% formaldehyde, 3% distilled glutaraldehyde, and approximately 0.45 mM $CaCl_2$ buffered to pH 7.4 with 0.1 M sodium cacodylate. After 2–3 min of local perfusion, the tissue was removed, minced, and immersed in fixative for 4–6 h at room temperature, or, in the case of sperm, it was removed from the ducts and placed immediately in the above fixative or in 1.5% distilled glutaraldehyde buffered to pH 7.4 with 0.1 M sodium cacodylate. (A few sperm preparations were fixed in a mixture of 1.5% glutaraldehyde and 4% tannic acid [35, 43], while others were treated with ruthenium red according to the method of Luft [31].) The tissues were washed overnight in 0.1 M sodium cacodylate buffer (pH 7.4) with 7% sucrose, followed by fixation for 2 h at 4°C in acetate-Veronal-buffered 1% OsO_4 (pH 7.4) with 5% sucrose. They were then treated for 1 h at room temperature with buffered 0.5% uranyl acetate containing 4% sucrose, quickly dehydrated in graded ethanols, and embedded in Epon 812.

For electron microscopy, silver-to-gray sections were cut with diamond knives on a Porter-Blum Sorvall MT-2 microtome (Ivan Sorvall, Inc., Norwalk, Conn.). The thin sections were collected on carbon- and Formvar-coated grids (Belden Mfg. Co., Chicago, Ill.), stained either with alkaline lead alone or with 5% aqueous uranyl acetate followed by lead, and examined with a Siemens IA electron microscope at 80 kV.

LABELING WITH CONCANAVALIN A AND HORSERADISH PEROXIDASE: Sperm freshly removed from the epididymis was thoroughly washed in an equal volume of 0.1 M phosphate-buffered saline at room temperature for 15 min. Concanavalin A (0.1 mg/ml saline) was added to each 50-μl aliquot of sperm in saline, and the solution was shaken for 15 min. Some suspensions were not treated with peroxidase, while others received 0.05 mg/ml horseradish peroxidase. The suspension was shaken for another 15 min at room temperature

before fixation in 3% phosphate-buffered glutaraldehyde (0.1 M, pH 7.4) at room temperature for 30 min. The sperm was then washed overnight in phosphate buffer and placed in a diaminobenzidine mixture (23) for 15 min. Thereafter, processing was routine except for the use of potassium ferrocyanide in the osmium tetroxide (24). Sperm mixed with concanavalin A alone was also incubated and osmicated in the same manner.

PREPARATION OF FREEZE-FRACTURE REPLICAS: For freeze-fracturing, small pieces of tissue, pellets of sperm, or oviductal contents mixed with pellets of sperm were placed in formaldehyde-glutaraldehyde fixative or 1.5% glutaraldehyde for 15–30 min and then immersed in 5–20% glycerol in 0.2 M cacodylate buffer or distilled water for 2–4 h. Pieces of tissue or pellets were mounted on cardboard disks, frozen rapidly in liquid Freon 22, and fractured in a Balzers 360 M apparatus (Balzers AG, Balzers, West Germany) with a stage temperature of −115°C. Some specimens were etched at −100°C for 1 min.

Electron micrographs of freeze-fracture replicas are generally mounted with the shadow from bottom to top, and all shadows are white.

PREPARATION OF SPECIMENS FOR SCANNING MICROSCOPY: Spermatozoa were critical point dried and vacuum evaporated with carbon and gold. Photomicrographs were taken on a JEM scanning microscope on Polaroid film.

OBSERVATIONS

Since the thin-section appearance of rat and guinea pig sperm has been adequately discussed by other investigators (12–16, 38, 39, 44, 50), only novel findings or factors relevant to correlation with freeze-fracture imagery will be presented here. Observations concerning freeze-fracture will take precedence, and, wherever possible, the structure of guinea pig and rat sperm membranes will be described in parallel fashion.

Appearance of the Head and Neck in Thin Sections

The heads of guinea pig and rat sperm are well endowed with components: the plasma membrane, the outer and inner acrosomal membranes, the acrosomal content, the nuclear envelope, and the nucleus containing condensed chromatin (Figs. 2, 4, 8).

Overlying the acrosome of the guinea pig sperm head, the plasma membrane tends to separate from the underlying acrosomal membrane except in regions of sperm rouleaux where the convex upper surface of each sperm closely apposes the concave undersurface of the adjacent sperm head (Figs. 1–3). Such laxity and irregularity of contour in the cell membrane over the acrosome are probably artifacts of specimen preparation. A delicate external coverlet or glycocalyx of variable thickness coats the plasma membrane. In routine preparations, this fragile coating is better preserved in the interstices between the stacked sperm heads than on exposed free surfaces. Although it generally looks amorphous, the glycocalyx is occasionally resolvable both in thin sections (Figs. 4 and 11) (8) and in replicas as fine, branching filaments. Its carbohydrate nature is indicated by its binding of concanavalin A (Fig. 3 *a*), horseradish peroxidase and concanavalin A, and ruthenium red.

In the region of closely contacting, stacked sperm heads, the usual filamentous glycocalyx appears to be lacking. The opposing membranes are precisely parallel, separated by an interspace of about 10 nm (Fig. 3 *b*) which is traversed by very evenly spaced linear densities, prompting Burgos et al. (8) to compare this specialization to the septate junctions of invertebrate epithelia. At high magnifications, the regularly repeating structures extending between the unit membranes are double faceted and distinctly lower in density than the membranes. Sections cut obliquely or tangential to the membrane surface display a highly ordered array of circular profiles (Fig. 3 *c*). It is not clear whether this lattice between the adhering membranes is a configuration peculiar to the glycocalyx or an unrelated surface specialization.

Abbreviations used in legends:

A, acrosome
AM, acrosomal membrane
AN, anulus
BP, basal plate
C, capitulum
JR, Jensens ring
M, mitochondrion
NE, nuclear envelope
PM, plasma membrane
SR, striated ring
1, coarse fiber 1
3, coarse fiber 3
8, coarse fiber 8

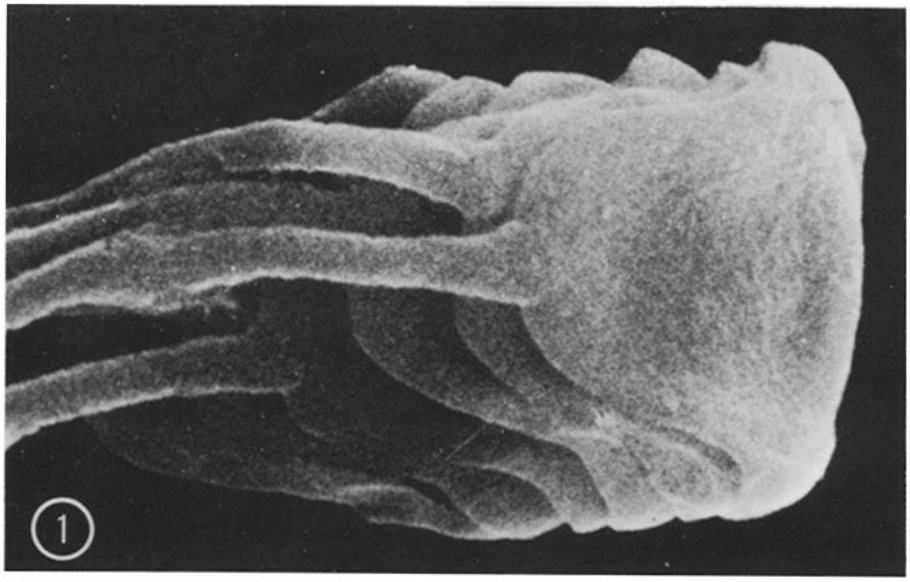

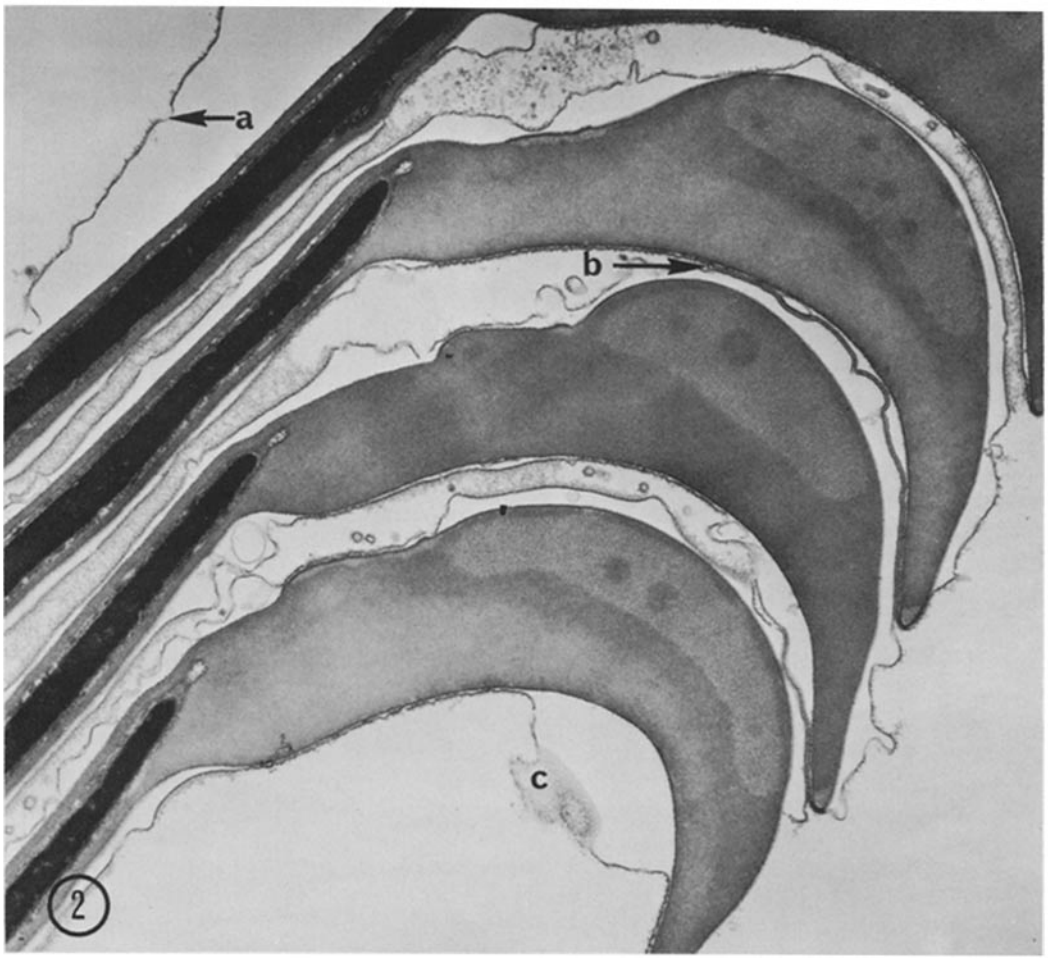

FIGURE 1 Scanning electron micrograph of a rouleaux of guinea pig sperm removed from the epididymis.

FIGURE 2 A comparable thin section through the acrosomes of stacked guinea pig sperm heads, depicting regions of loose and firm attachment. The letters *a*, *b*, and *c* refer to corresponding areas at higher magnification in Fig. 3. A glycocalyx covers the external surface in all regions of the plasma membrane of the head. × 19,800.

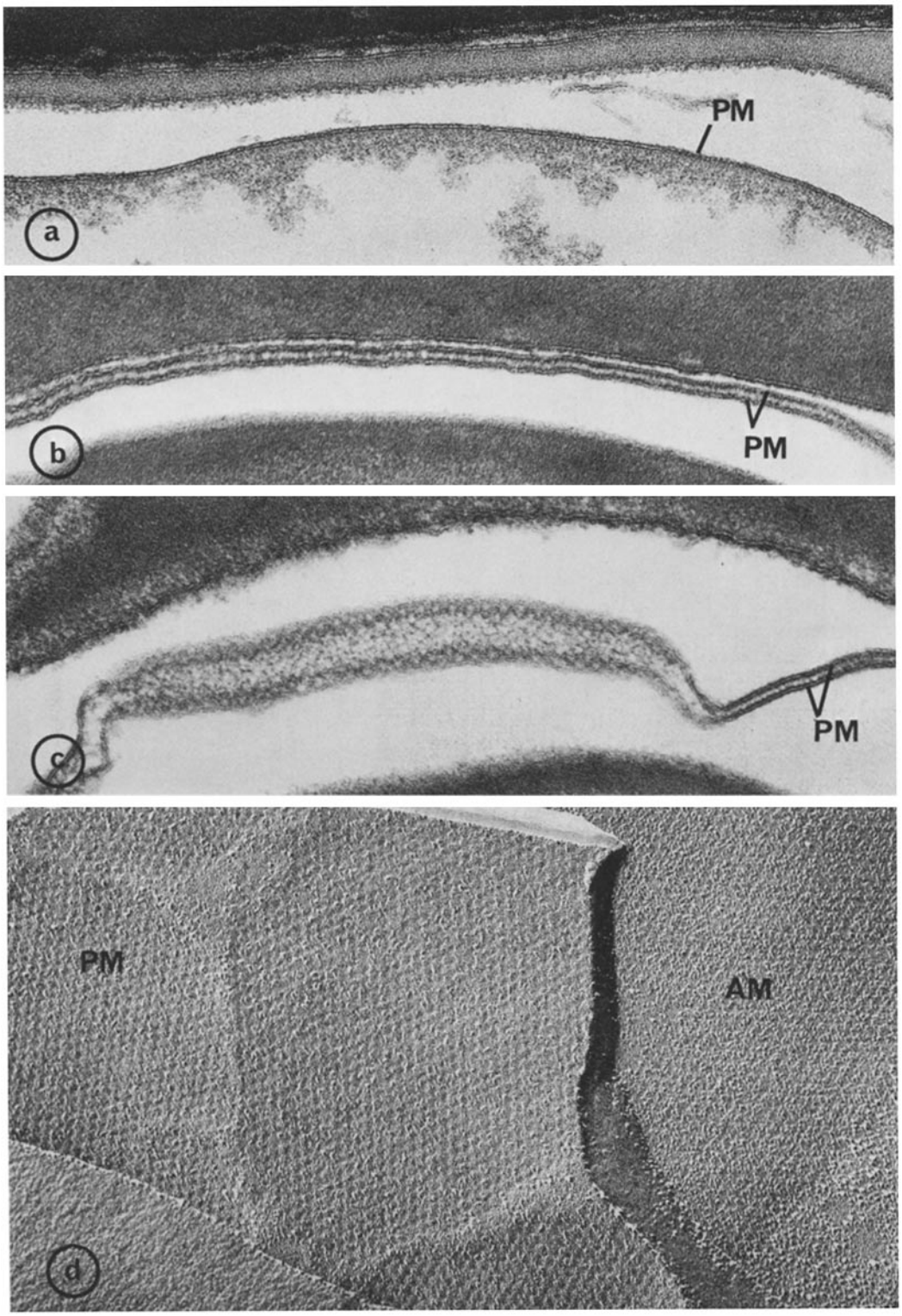

FIGURE 3 Guinea pig. *a*: concanavalin A uniformly binds to the glycocalyx, obscuring its substructure. Fig. 3 *b*: in areas of close attachment, periodic tubular striations are observed between the membranes. Fig. 3 *c*: tangentially cut sections resemble a series of contiguous circles. Fig. 3*d*: in freeze-fracture preparations, the areas of plasma membrane (*PM*) corresponding to those with highly organized glycocalyces in thin section have a quilted pattern on the A face. *AM*, (presumed) acrosomal membrane. Fig. 3 *a*, × 62,500; Fig. 3 *b*, × 100,000; Fig. 3 *c*, × 85,000; Fig. 3 *d*, × 78,000.

A fibrous, periodic layer beneath the plasma membrane and posterior to the acrosome constitutes the postacrosomal dense lamina (12), best observed when the sperm is stained at 40°C for 12–16 h in 0.5 M uranyl acetate en bloc (Fig. 8).

Centrally, the tail attaches at a nuclear recess, the implantation fossa (Figs. 8, 10, 13, 16). Proceeding from behind the nucleus, it is composed of a partially fused nuclear envelope and a dense, amorphous basal plate from which fibrils extend to the capitulum (Figs. 13 and 16). Sideways, between the basal plate and the striated ring, where the plasma membrane either fuses with the nuclear envelope or intimately approaches it (Fig. 16), is a geometric array of nuclear pores rarely visible in thin section. The partly fused portion of the envelope resembles a gap junction in morphology, i.e., two parallel unit membranes separated by a 2–4-nm gap (Fig. 18 *b*).

Appearance of the Freeze-Fractured Head

In the plasma membrane, the two fracture faces are distinguished according to their relationship to the cytoplasm and extracellular space (6). The inner fracture face of the membrane (face A) is adjacent to the cytoplasm, while the outer fracture face (face B) is adjacent to the extracellular space. The A face is ordinarily rich in membrane particles; the B face contains depressions. With respect to fractures of internal membranes in this study, the fracture face closest to the cell axis is designated face A and the face closest to the plasma membrane, face B.

PLASMA MEMBRANE: For the most part, the plasma membrane of the rat sperm head is devoid of geometric arrays (Fig. 10). Not so in the guinea pig: extensive sites of the guinea pig plasma membrane which correspond to the previously described areas of highly organized glycocalyx have a quilted pattern in freeze-fracture (Figs. 3 *d* and 5). In organization this quilted lattice precisely imitates that of the alveolate cell-coat seen in a tangential thin section (Fig. 3 *c*). The presence of the pattern in the membrane fracture faces marks this structure as an integral part of the membrane. The arrangement of the patterned areas in plaques is a notable feature (Figs. 3 and 5). A similar geometric pattern is present in small areas of the rat sperm (Fig. 6). Adjacent and intervening zones of the membrane contain scattered particles and depressions. (More detailed descriptions of this membrane are provided in the figure legends.)

In addition to the quilted pattern, a saw-toothed elevation, such as that described by Koehler (25) in the rabbit, rises from the posterior margin of the equatorial segment in the guinea pig (Figs. 7 and 8). Caudal to this corrugated region, well-ordered geometric arrays of particles within depressions are occasionally found in the B face of the plasma membrane overlying the postacrosomal dense lamina (Figs. 8 and 9). Fine, filamentous particles, as well as spherical ones, also characterize this region (Fig. 7). A circumferential groove in the plasmalemma demarcating the boundary between the head and neck is prominent in both guinea pig and rat sperm (Figs. 10 *a*, 15–17). In freeze-fracture preparations, the depths of the groove show a very fine transverse striation, hence the term "striated ring." The ring is separated from the particle-rich areas of the membrane by a smooth terrain interrupted only by several linear aggregates of particles (A face) or depressions (B face) (Fig. 15).

ACROSOME: In the rat, the acrosomal material is first observed in crystalline form (Fig. 11) in the rete testis and caput epididymis. Congruently, an ordered, hexagonal pattern is visible in the membrane (Fig. 12). In both the rat and guinea pig, the hexagonal configuration is visualized as an extensive sheet with many random membrane particles nearby in other portions of the acrosomal membrane (Figs. 5 and 12). The patterned areas in the guinea pig acrosomal membrane, unlike those of the rat, do not overlie any visibly crystalline material. In both, however, A and B faces can be identified.

NUCLEAR MEMBRANE AND IMPLANTATION FOSSA: In both the guinea pig and rat, membranes of the nuclear envelope cephalad to the striated ring are noteworthy only for lacking nuclear pores and for fracturing in an extremely variegated geometric pattern, the fracture frequently skipping from one membrane to the other (Fig. 5). Behind the striated ring, however, the nuclear envelope assumes intriguing variations in structure. The zone between the basal plate and the striated ring contains closely spaced and precisely ordered nuclear pores (Figs. 15 and 17). A smooth and relatively particle-free region of the nuclear envelope covers one portion of the basal plate, while the other half contains large particles and complementary depressions (Figs. 9, 14, 18). In the rat (Fig. 17), the particles are approximately 15 nm in diameter, with varied spacing up to 20 nm apart. In the guinea pig, where this highly organized aggregate is especially prominent, the parti-

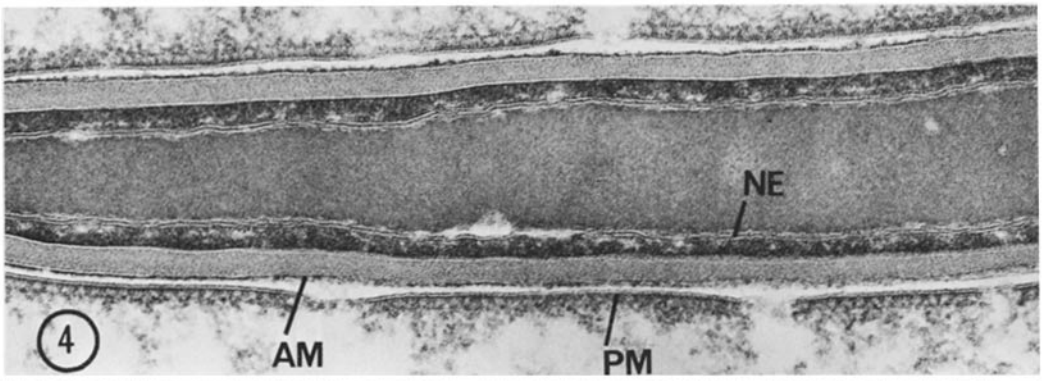

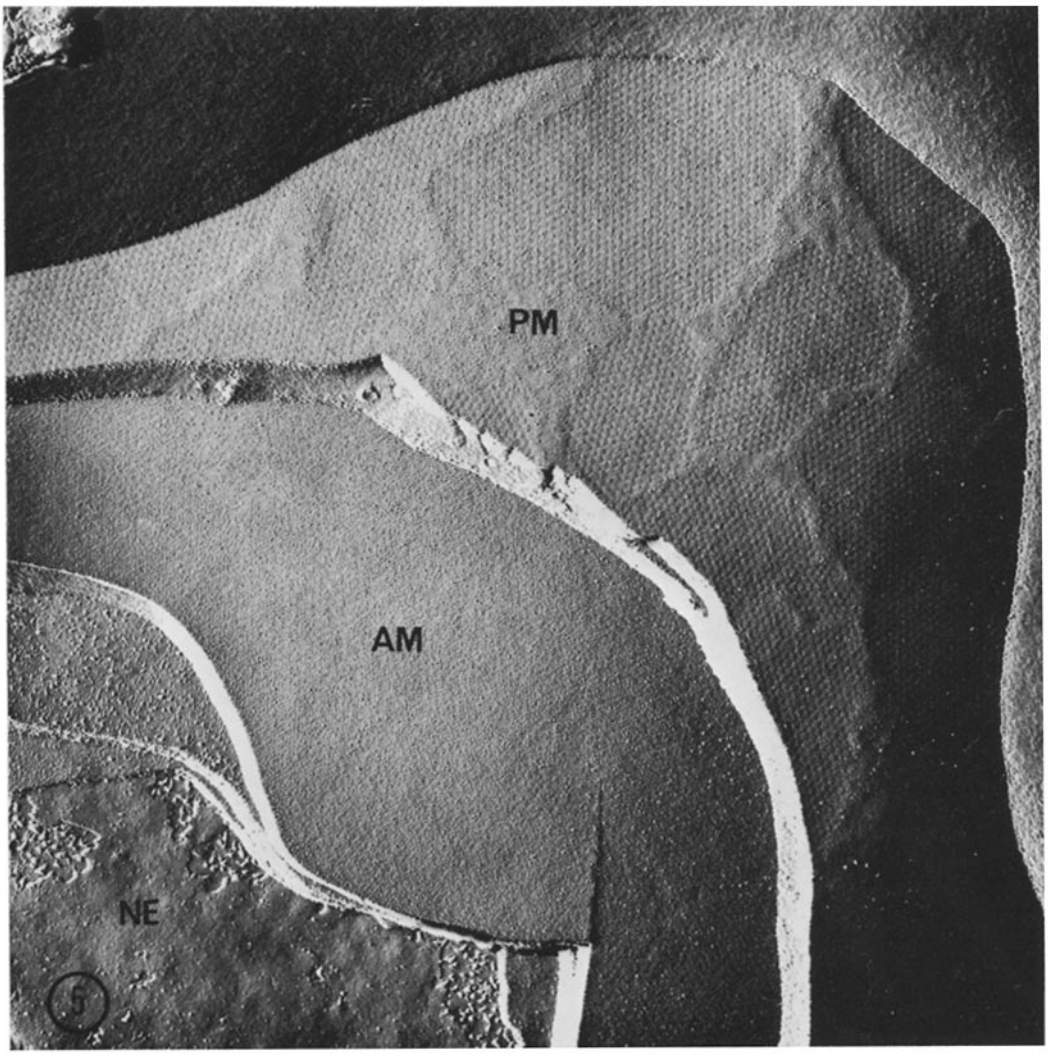

FIGURE 4 Guinea pig sperm. Tannic acid (4%)-glutaraldehyde fixation accentuates the organization of the glycocalyx of the plasma membrane (*PM*) into domains. Note the close approximation of the membranes of the nuclear envelope (*NE*). *AM*, acrosomal membrane. × 73,000.

FIGURE 5 Guinea pig sperm. Freeze-fracture reveals the quilted pattern of the plasma membrane in domains as well. Intervening areas are relatively smooth, with few membrane particles. What we presume to be the acrosomal membrane (*AM*) has a more uniform but similar pattern. The pore-free nuclear envelope (*NE*) always fractures in variegated fashion. *PM*, plasma membrane. × 36,000.

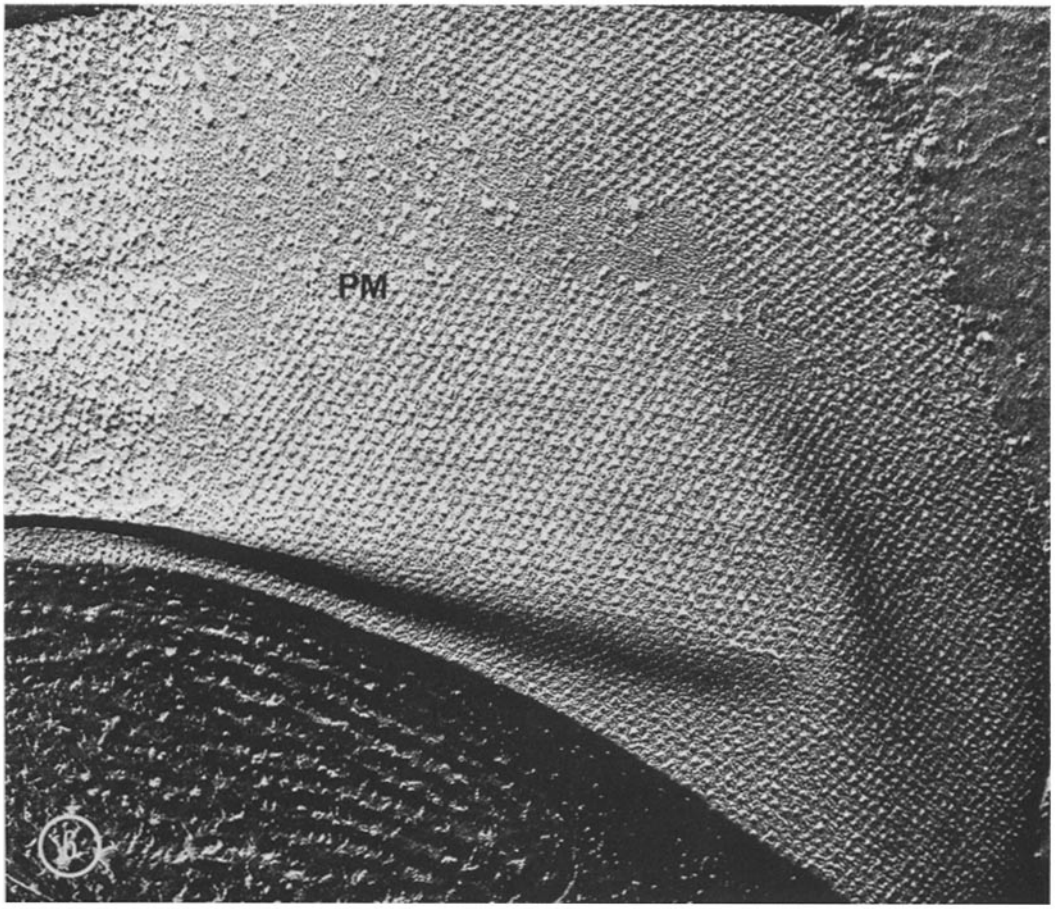

FIGURE 6 In the rat, although no highly organized glycocalyx is visible in thin sections of the plasma membrane, freeze-fracture discloses domains of particles in hexagonal array. The ordered, condensed nuclear content is evident (lower left). *PM*, plasma membrane. × 140,000.

cles are 15–25 nm in diameter, usually with 20-nm spaces between. Ordinarily the particles are found in the B face (inwardly directed outer half) of the nuclear envelope, while indentations occupy the outer leaflet of the nuclear membrane itself (Fig. 18 *a*). Whether the particles completely traverse both membranes is not clear, but they are probably shared by both, which would account for the scalloped appearance in thin section (Fig. 18 *b*). This region neighbors the basal plate which serves to anchor fibers extending from the connecting piece. (The orderly arrangement of particles at the implantation fossa develops relatively early and is observed in spermatids before nuclear condensation occurs.)

TAIL: THIN SECTION—MIDPIECE (MITOCHONDRIAL SHEATH): In the midpiece, the plasma membrane is closely applied to the gyres of the mitochondrial helix that overlies the outer dense fibers and the central axonemal complex. In the guinea pig, tannic acid fixation accentuates an otherwise vague periodicity (absent in the rat) in the space between the mitochondria and plasmalemma (Fig. 19). In both guinea pig and rat, a fusiform, 2–5-μm cytoplasmic droplet containing an heterogeneous assortment of vesicles and stacks of flattened membranes separates the mitochondrial membrane from the plasma membrane. In the guinea pig the droplet is found midway; in the rat it is usually situated farther back near the anulus.

Where the mitochondrial sheath of the midpiece joins the fibrous sheath of the principal piece, the anulus (Jensens ring) intervenes. The overlying

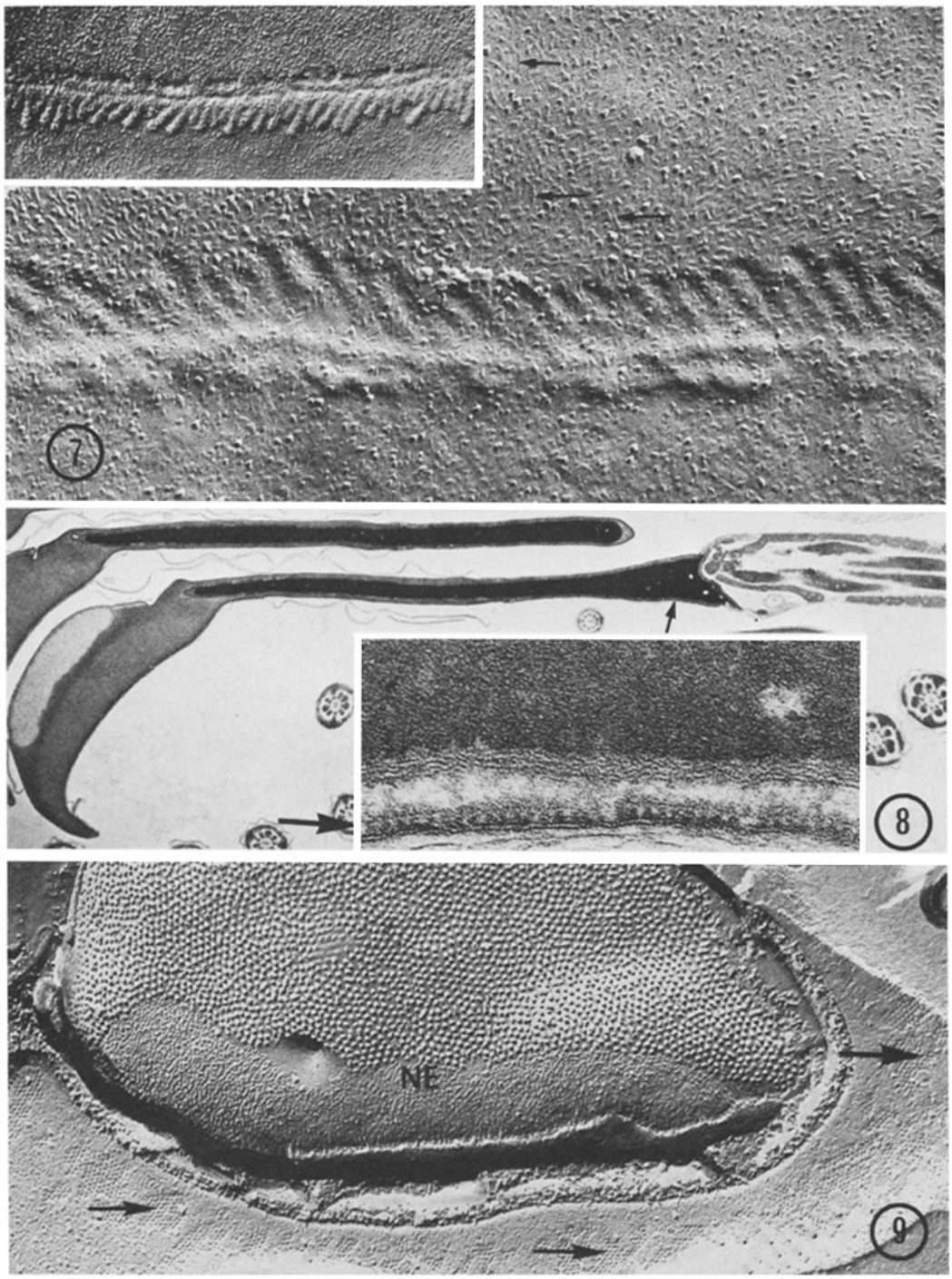

FIGURE 7 Guinea pig sperm. Posteriorly, at the distal margin of the equatorial segment of the acrosome, the plasma membrane has a serrated pattern of oblique rods visualized as alternating elevations and depressions. Near the rods' free ends, short fibrillar profiles (arrows) are common in the membrane. Note their absence on the alternate side of the serration. × 102,000; *inset*, × 38,000.

FIGURE 8 Guinea pig sperm. The *inset* is a high-magnification view of the postacrosomal dense lamina (arrow) in the area indicated by the arrow in the main figure. × 7,000; *inset*, × 100,000.

FIGURE 9 The **B** face of the plasma membrane in this region of guinea pig sperm shows honeycomb arrays of particles within depressions (arrows). This region of the sperm plasma membrane is caudal to that which makes initial contact with the oolemma. The characteristic freeze-fracture appearance of the nuclear envelope (*NE*) limiting the implantation fossa is described in subsequent figures. × 38,000.

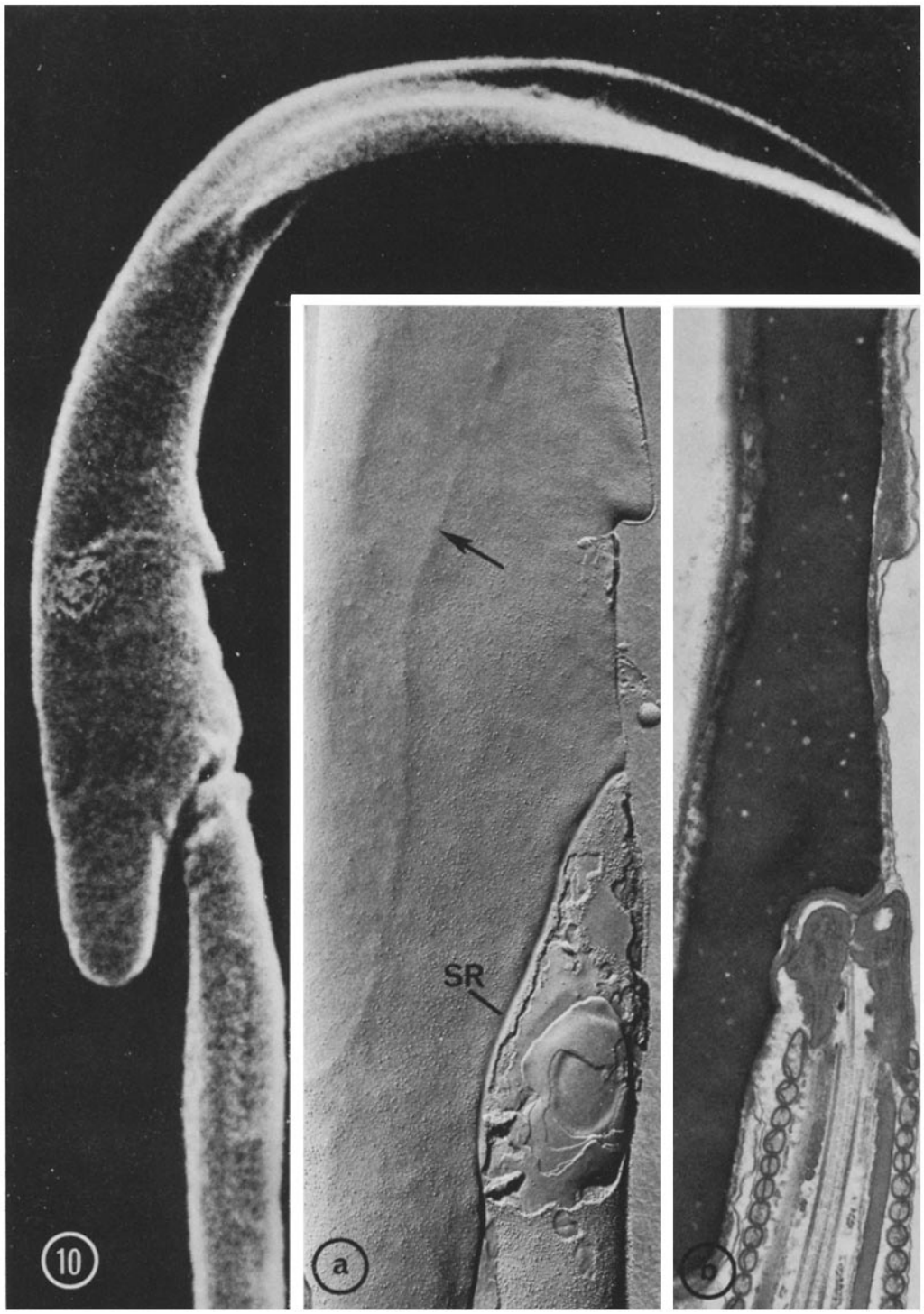

FIGURE 10 Scanning electron micrograph, freeze-fracture (Fig. 10 *a*), and thin section (Fig. 10 *b*) of rat sperm, showing the juncture of the head and tail. In the freeze-fracture preparation, a striated ring (*SR*) marks this juncture. The posterior limit of the acrosome (arrow) is also reflected in the plasma membrane. Fig. 10 *a*, × 24,000; Fig. 10 *b*, × 18,000.

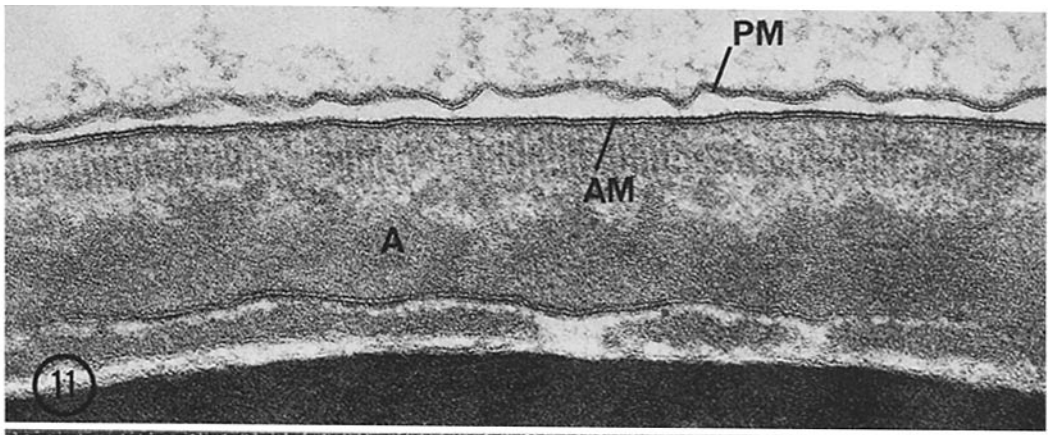

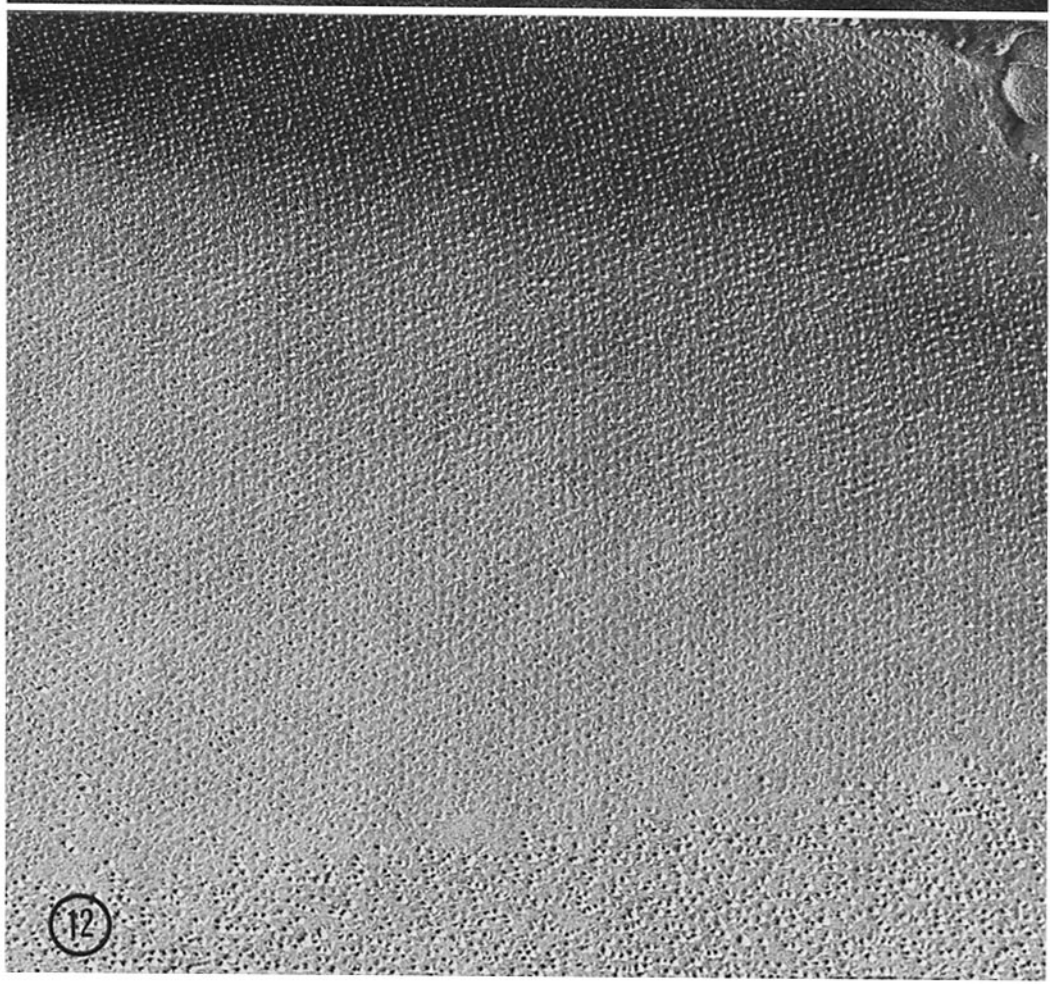

FIGURE 11 Sagittal section of rat sperm head illustrating portions of the plasma membrane (*PM*), acrosomal membrane (*AM*), subacrosomal density, and nucleus. Part of the acrosome (*A*) underlying the outer acrosomal membrane is crystalline. × 100,000.

FIGURE 12 Rat sperm. An A face through a region of the membrane (presumably acrosomal) which contains heterogeneous particles in hexagonal pattern. Where the pattern disappears (in the lower portion of the micrograph), numerous 9–10-nm membrane particles are visible. × 75,000.

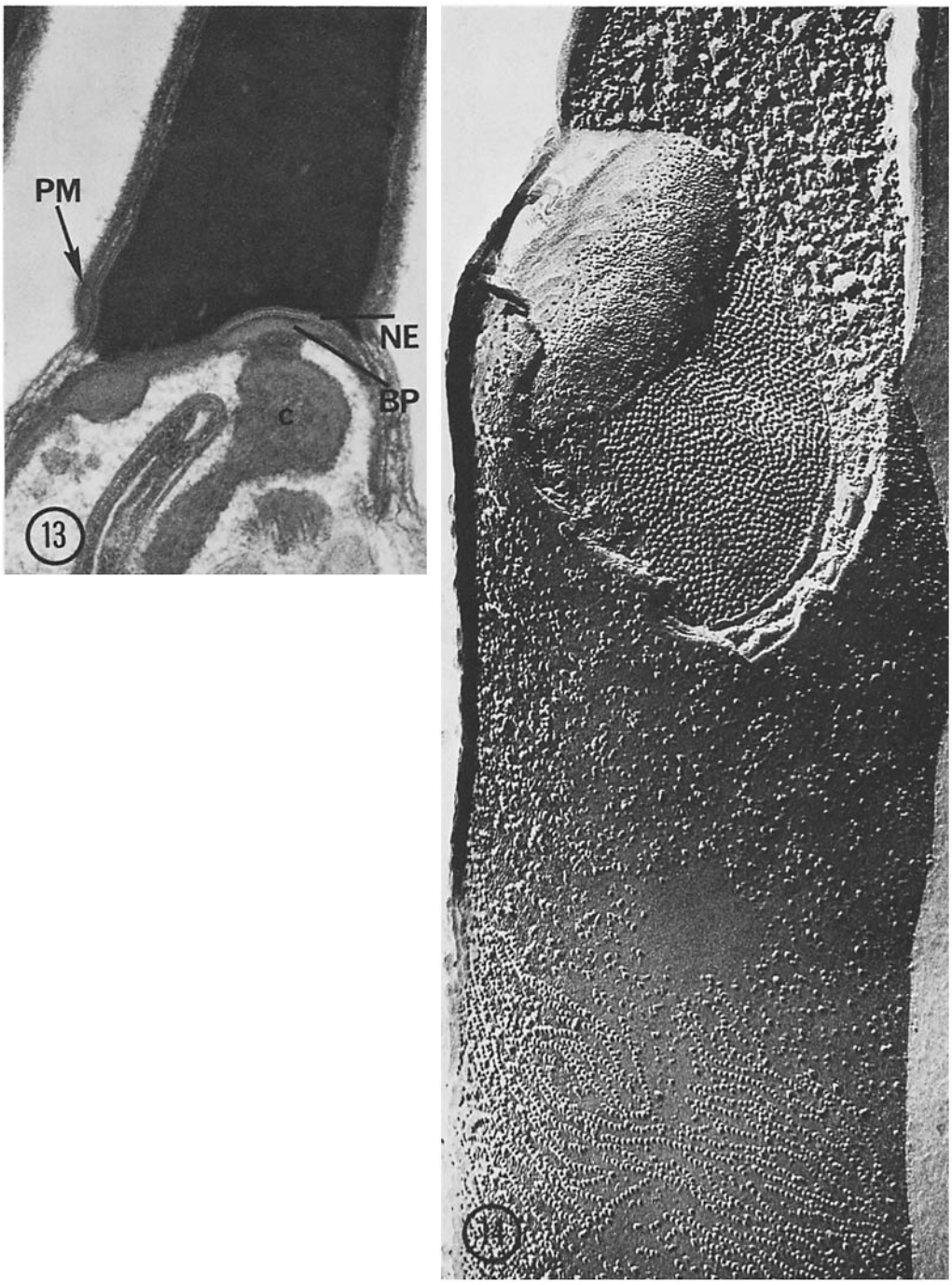

FIGURES 13 and 14 This sagittal section of the neck of guinea pig sperm (Fig. 13) and a comparable freeze-fracture image (Fig. 14) are placed here for orientation to Figs. 15–18. The plasma membrane (*PM*) is continuous over the head, neck, and tail and comes into close contact with the nuclear envelope (*NE*) at the level of the striated ring. The posteroventral portion of the nuclear envelope, overlying an area of fibrous attachment between the capitulum (*C*) and the basal plate (*BP*), reveals an array of large particles in freeze-fracture. The contiguous area of the nuclear envelope is smooth. Strands of particles in the plasma membrane (lower part of Fig. 14) mark the beginning of the mitochondrial sheath of the midpiece. Fig. 13, × 26,500; Fig. 14, × 87,000.

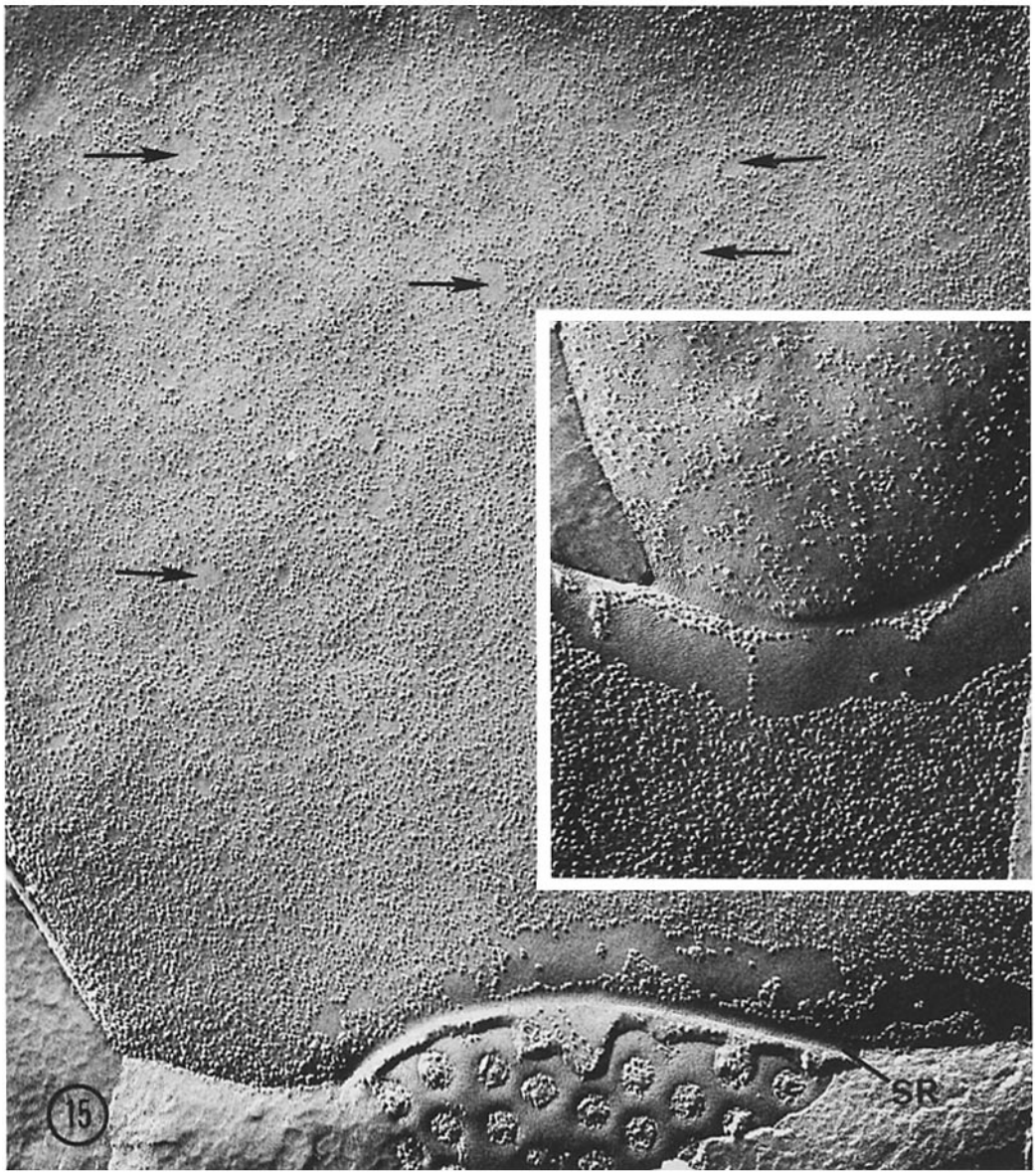

FIGURE 15 Guinea pig sperm. In the particle-rich plasma membrane of the head anterior to the striated ring (*SR*), anular configurations (arrows) are common. Immediately in front of the striated ring, the A face is always smooth save for isolated rows of particles. In the inset, the plasma membrane of the initial portion of the tail (upper half) is intact. In the main figure, it is absent, revealing a smooth fracture face A of the outer nuclear membrane and pores of the nuclear envelope. Fig. 15, × 56,000; *inset*, × 66,000.

plasma membrane is firmly bound to the ring and clings to the fibrous sheath (Fig. 24). As observed in cross-section (particularly in the guinea pig), the plasma membrane reveals a focal increase in density and an apparent attachment to the fibrous sheath opposite coarse fiber 1 (Fig. 27). This asymmetry of the tail is similar to that in the earthworm (5). The symmetrical attachments between fibers 3 and 8 and the longitudinal fibers have long been recognized (5, 7). In the endpiece varying patterns of microtubules are encased by the plasma membrane.

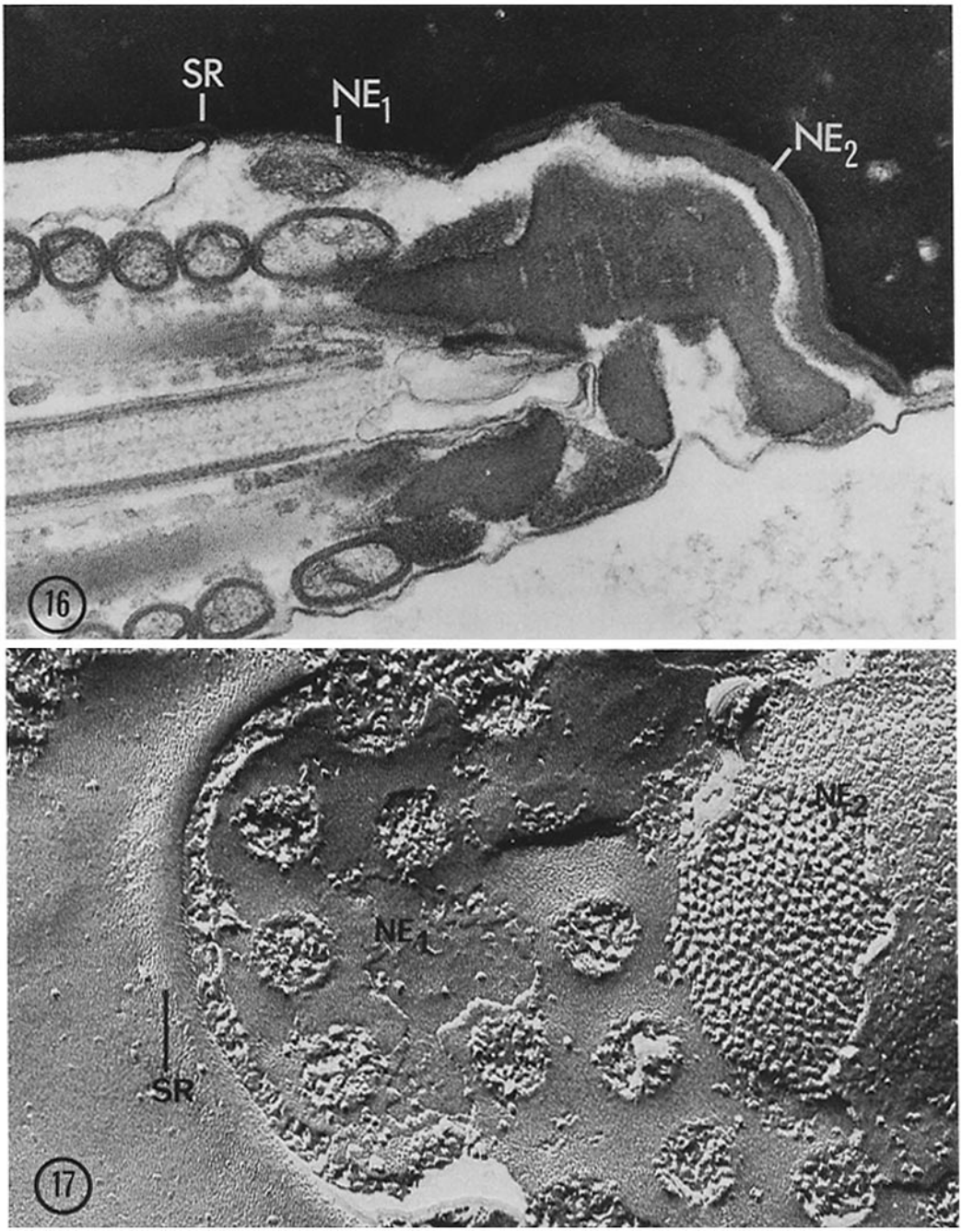

FIGURES 16 and 17 Sagittal section through the neck region of rat sperm (Fig. 16), and a fracture preparation of the nuclear envelope in the same region (Fig. 17). Nuclear pores pierce that area of the envelope (NE_1) which lies between the indentation of the striated ring (SR) and the basal plate. The nuclear envelope (NE_2) overlying the ventral part of the plate has a patch of large particles. As in the guinea pig, the membranes of the nuclear envelope adjacent to the area of large particles are relatively smooth. Fig. 16, × 50,000; Fig. 17, × 100,000.

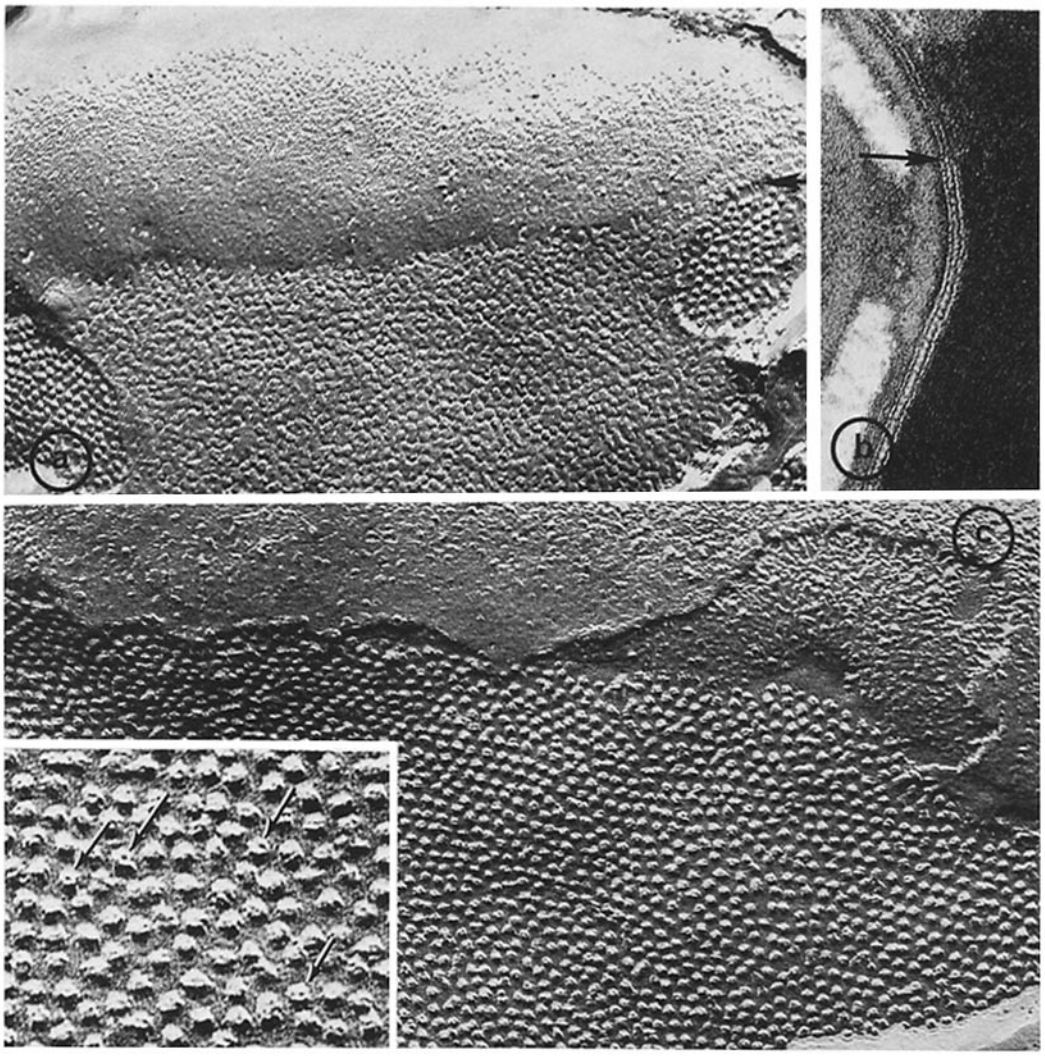

FIGURE 18 Fig. 18 *a*: a fracture through the nuclear envelope overlying the basal plate in guinea pig sperm. Arrays of large particles occupy the B face of the outer nuclear membrane, and indentations are centrally located in the outer leaflet of the nuclear membrane proper. As in the rat, the dorsal portion of the nuclear membrane is smooth. The arrow denotes the intersection between particulate and smooth portions of the nuclear envelope. Fig. 18 *b*: the arrow corresponds to the same intersection shown in Fig. 18 *a*. Above the arrow, the nuclear envelope has a 2–4-nm interspace; below the arrow, the interspace is more than 15–25-nm wide. Fig. 18 *c*: the large particles of the nuclear envelope composing the implantation fossa are seen here to be coplanar with the smooth portion of the membrane. The *inset* shows the indentations or channels (arrows) in the particles to advantage. Also note the struts emanating from some of the particles. Fig. 18 *a*, × 70,000; Fig. 18 *b*, × 60,000; Fig. 18 *c*, × 96,000; *inset*, × 160,000.

FREEZE-FRACTURE: The A face of the plasma membrane of the guinea pig midpiece discloses circumferential arrays of 6–8-nm particles, and the B face discloses strands of depressions wherever the membrane overlies the gyres of the mitochondrial helix (Figs. 20–23, 25). Conversely, the membrane covering interstices between mitochondria reveals only sparse, 8-nm particles. These beaded strands of particles terminate abruptly at the anulus (Figs. 24 and 25) and

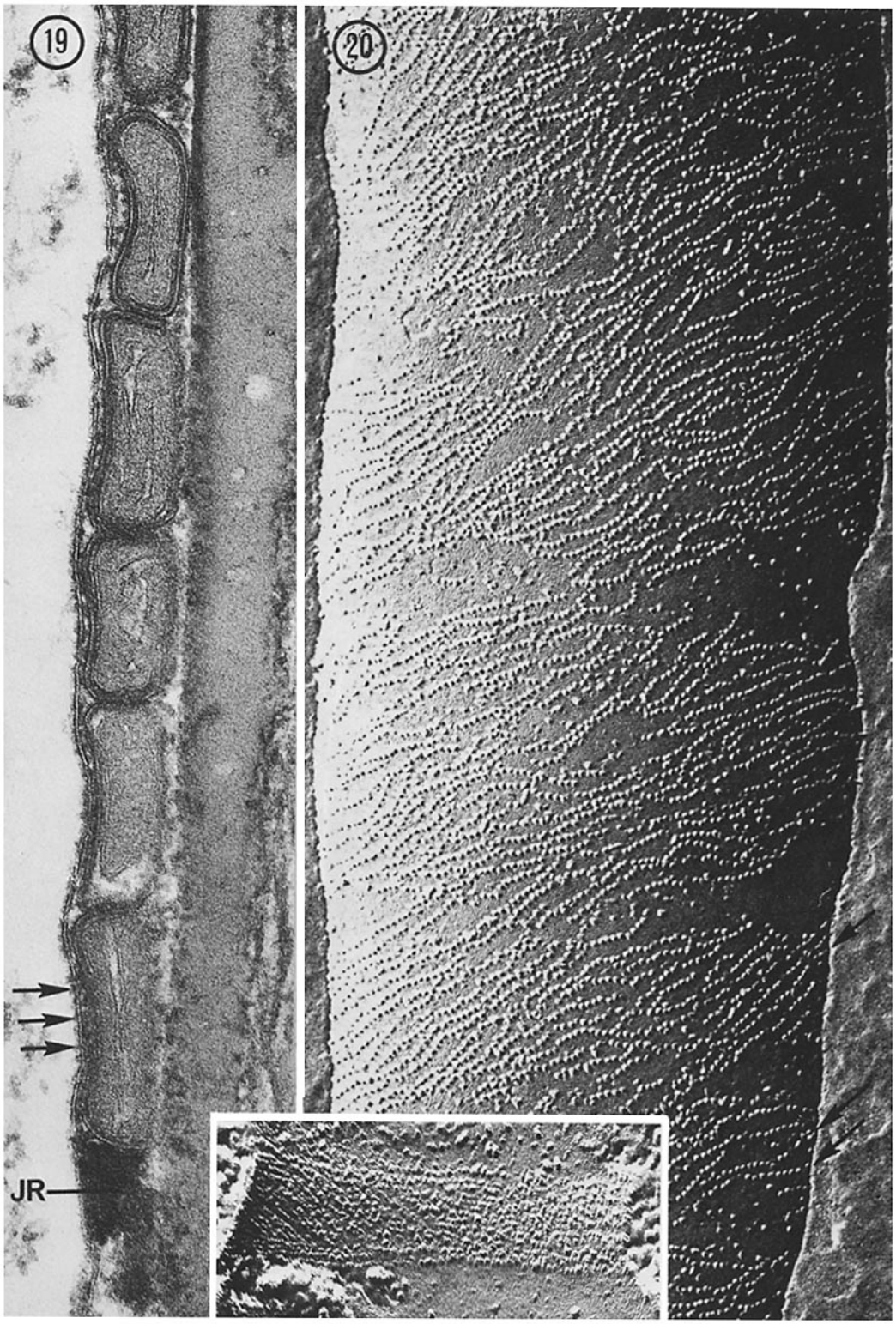

FIGURES 19 and 20 Longitudinal section (Fig. 19) and fracture (Fig. 20) through the midpiece and anulus (Jensens ring, *JR*), respectively, of the guinea pig sperm tail. Tannic acid-glutaraldehyde fixation accentuates a faint periodicity between the mitochondrial and plasma membranes in thin section (arrows) (Fig. 19). These particles are 6–8 nm in diameter in freeze-fracture. Smooth areas between the sheaths of particles correspond to spaces between mitochondria. The angle of the strands (arrows) is similar to that of the mitochondrial helix. In freeze-fracture, the plasma membrane overlying Jensens ring is roughened (*inset*). Fig. 19, × 96,000; Fig. 20, × 96,000; *inset*, × 90,000.

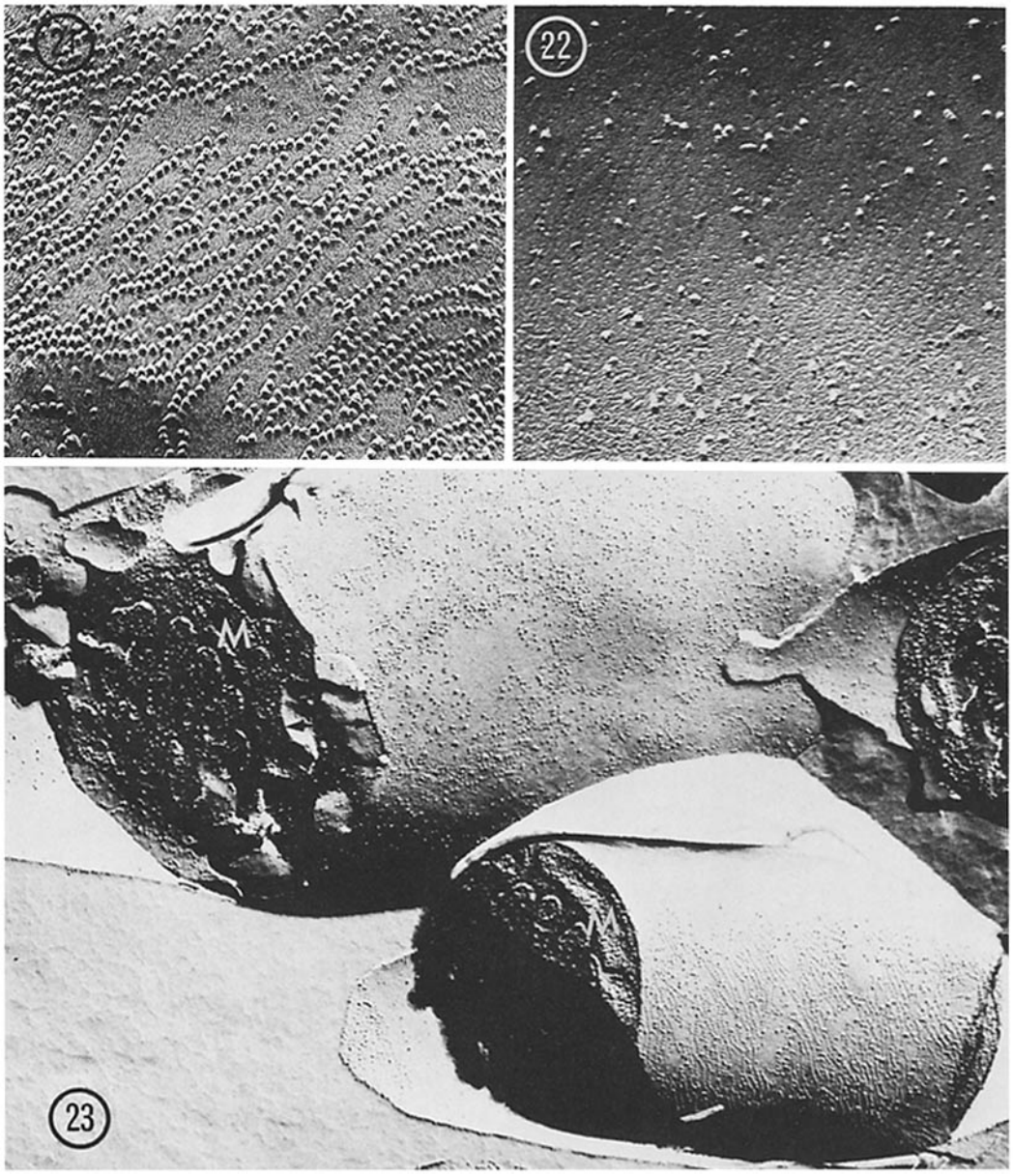

FIGURES 21 and 22 Fracture faces A (Fig. 21) and B (Fig. 22), respectively, of the guinea pig midpiece plasma membrane expose the strands of particles and pits. Fig. 21, × 120,000; Fig. 22, × 105,000.

FIGURE 23 Guinea pig sperm. The particulate strands are absent in the region of the cytoplasmic droplet where the plasma membrane and mitochondria (*M*) are separated (arrows), as seen in the upper sperm. Where the membrane is in close contact with a mitochondrion (*M*, lower sperm), however, the strands are invariably present. × 40,000.

less abruptly at the neck and cytoplasmic droplet. Similarly, the membrane enclosing the cytoplasmic droplet lacks any strands of particles (Fig. 23), nor does the plasma membrane of the rat midpiece generally manifest such particles.

At the anulus, the fracture faces of the membrane are roughened and hence are easily distinguished by freeze-fracturing (Figs. 20 (inset) and 25). They vary in appearance from merely a rough-textured background overlain with a few

large particles to one with a heavy conglomerate of large and small, thread-like particles.

In guinea pig sperm, the proximal portion of the principal piece contains a double row of staggered 9-nm particles (a "zipper") which courses longitudinally over the ribs of the fibrous sheath opposite fiber 1 (Figs. 26 and 28); this is the same site visualized in thin section as an attachment between the plasma membrane and fibrous sheath (Fig. 27). Identically located in the rat, a single strand of widely spaced 8–9-nm particles is present, and in both species, the longitudinal arrays terminate before reaching the endpiece. In both, too, this membrane differentiation can be found in late spermatids in the testis and thus is not a late differentiation associated with maturation in the epididymis.

A subpopulation of guinea pig spermatozoa, particularly those which achieve motility during incubation in a nutrient medium or in physiological saline, displays a linear array of large particles throughout the principal piece. (See Table I for summary of freeze-fracture observations.)

DISCUSSION

An Overview

Freeze-fractures of the plasma membrane of guinea pig sperm reveal a remarkable diversity of structure within an otherwise commonplace unit membrane. The plasma membrane of the head has discoid areas of a highly ordered "quilt" adjacent to localities rich in randomly dispersed particles. Within the particle-rich areas, rosettes unrelated to any known endocytic or exocytic activity are visible in this fully differentiated cell, and a sharply delineated region in front of the posterior ring is markedly smooth except for uniform arrays of particles within depressions on fracture face B. In the midpiece, strands of small particles appear only where the membrane snuggles close to mitochondria. The anulus segregates these strands from the larger particles of the principal piece, where a big particle zipper overlies only fiber 1. Linear arrays of similar particles are rarely found.

How close a correlation exists between these fracture face specializations and various regional functional specializations is not yet known, but the fact that major structural specializations *do* exist provides an impetus to further exploration of membrane functions. Perhaps such patterns can even be utilized to identify specific areas of the membrane after cell fractionation.

The guinea pig plasma membrane is indeed a rich model for investigating the control of membrane patterns in general. What factors are responsible for maintaining interfaces between distinctly different particle populations? Is the membrane matrix uniformly fluid or do unknown barriers segregate different types of particles and patterns? Are certain patterns, governed by physicochemical properties, common in the architecture of many systems and yet fulfill very disparate functions? The recognition and definition of these differences with the use of a continuous membrane would doubtless help to unveil these mysteries.

Acrosome and Plasma Membranes

Evidently the geometric pattern in the acrosomal membrane is a feature common to many species (25, 26, 40). Other observers have reported that this pattern is confined to the paranuclear portion of the invaginated acrosomal sac. In rat and guinea pig sperm, however, the pattern is not thus clearly circumscribed. Particularly in the rat, the orderly array is apparently associated with the crystalline portion of the acrosomal content and is most prominent near the outer part of the acrosomal membrane; the pattern itself is not made up of elements identical to what are considered ordinary membrane particles. Unlike the adjacent clusters of particles, those in areas of linear or hexagonal design are discoid, less regular in contour, and smaller.

The analogous architecture of the acrosomal crystal and the patterned membrane suggests that the two structures are kindred. In fact, the array in the membrane may well be either a reflection of the crystal or enzymes such as hyaluronidase or a trypsin-like protease (22) which presumably help the sperm to penetrate the cumulus oophorus and zona pellucida, respectively. It is also intriguing to speculate that a crystalline enzyme might reside in the membrane and diminish during the release of proteases at the time when sperm penetrates the zona pellucida (13, 27).

That a similar pattern exists within guinea pig, and other (25, 26) acrosomal membranes lacking any visible crystalline material after ordinary preparative procedures, detracts from the concept that the pattern is created by a crystal imprint on the pliable unit membrane. The polar portions of mouse eosinophil granule membranes (unpublished observations) and membranes limiting crystalline yolk (30) display no such membranous imprint of their content. Furthermore, the apical

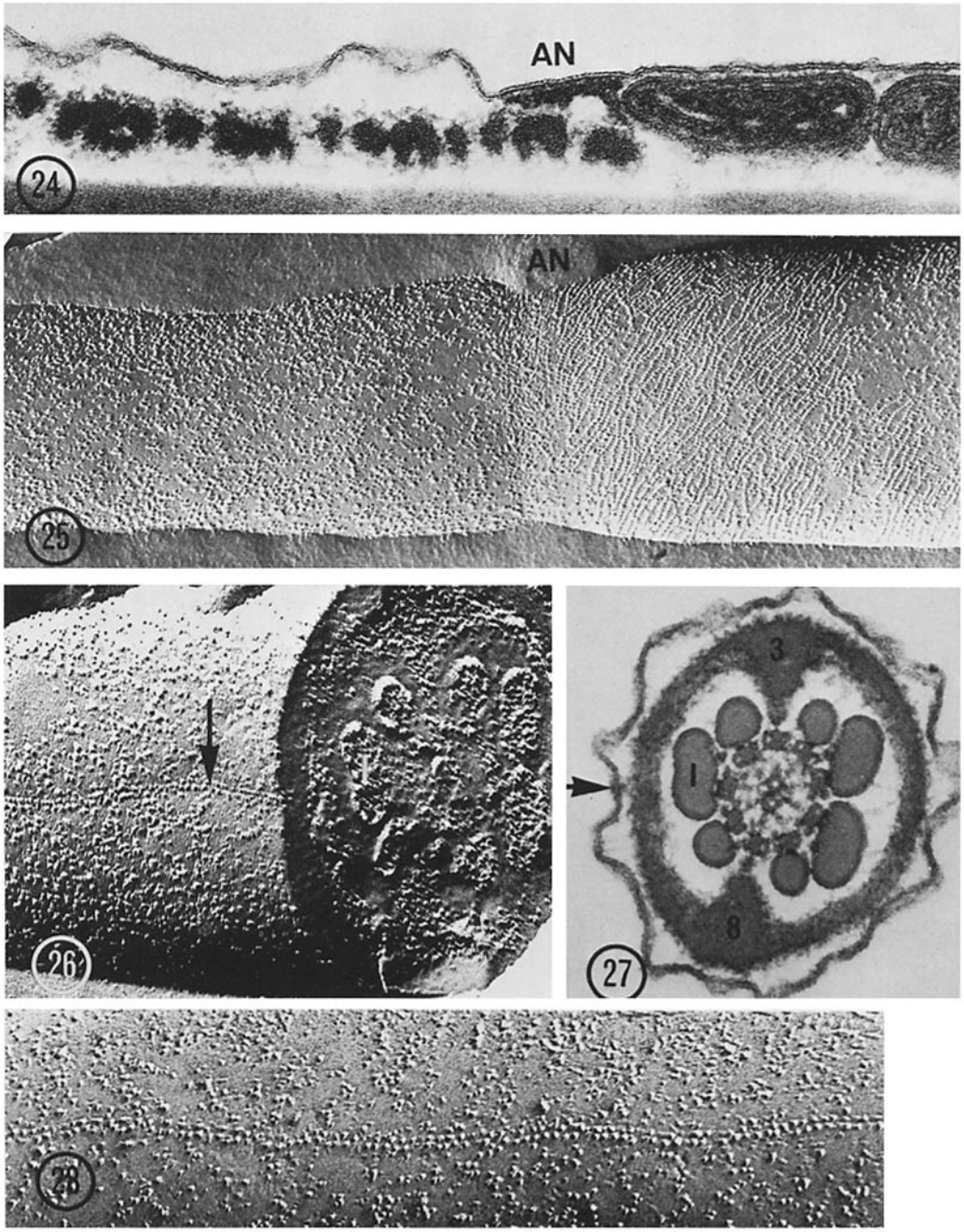

FIGURES 24 and 25 Guinea pig sperm. The strands of particles end abruptly at the anulus (*AN*), coincident with the termination of the mitochondrial helix. In the principal piece, the particles are heterogeneous in size, with the majority much larger than those comprising the strands. Fig. 24, × 48,000; Fig. 25, × 76,700.

FIGURES 26–28 Freeze-fracture and cross section of the guinea pig principal piece. A punctate density (arrow) (Fig. 27) appears to fasten the plasma membrane to the fibrous sheath opposite outer coarse fiber *1*. Attachment between the fibrous sheath and outer doublets of the axoneme is evident at *3* and *8*. The longitudinal double row of large particles (arrow) (Figs. 26 and 28) contained in the plasma membrane corresponds to the point of attachment opposite fiber *1* seen in thin section. This large, undulating, particulate zipper is likely to be found in the sperm tails of many species (see text). Fig. 26, × 76,000; Fig. 27, × 76,000; Fig. 28, × 98,000.

TABLE I

*Comparison of Freeze-Fractures of Guinea Pig and Rat Epididymal Sperm**

Location	Observation	Guinea pig	Rat
Head			
Plasma membrane	Domains of particles in hexagonal array over acrosome	++	+
	Palisade of elevations over equatorial segment	++	−
	Rectilinear arrays over postacrosomal dense lamina	+	−
	Striated ring at junction of head and neck	++	++
	Smooth area anterior to striated ring	++	++
Acrosome	Fine hexagonal pattern	++	++
Nuclear envelope	Variegated fractures, no pores	++	++
Neck			
Nuclear envelope, "redundant portion"	Precisely ordered nuclear pores	++	++
Implantation fossa	Large (15–25 nm) particles in B face of nuclear envelope	++	++
Tail-Plasma membrane			
Midpiece	Linear strands of 6–8-nm particles	++	−
Anulus	Rough textured	++	+
Principal piece	Double row of staggered 9-nm particles (the zipper)	++	+

* ++, prominent; +, present; −, not observed.

plasma membrane of the urinary bladder epithelial cell in the rat (41), like portions of the plasma membranes of guinea pig and rat sperm heads, exhibits a distinctive hexagonal pattern, without underlying crystals. However, one feature that the apical membrane of rat bladder transitional epithelium, the acrosomal membrane, and the plasma membrane of the sperm head share is a facile expansion of surface area. In the epithelial cell, the surface area distends along with the bladder; in sperm, the acrosomal and plasma membranes might stretch before acrosomal disruption, a relatively vast expansion in surface dramatically and simply demonstrated by incubating sperm in distilled water for 10 min (unpublished observations). Consequently, the hexagonal arrays of these three membranes may be a result of the tight packing of membrane constituents, which then rapidly move apart for membrane expansion. At the moment, both theories seem reasonable, i.e., that the crystalline pattern represents a membrane-associated enzyme, or that it reflects a structural unit of the membrane required for fast membrane expansion.

Equatorial Segment

Overlying the equatorial segment of the acrosome in the guinea pig, the plasma membrane exhibits a serrated pattern of oblique elevations varying in length and suggesting the presence of underlying parallel rods, each with one end fixed to the posterior margin of the acrosome and the free end presumably oriented toward the tip of the sperm head. These superficially resemble the triangular profiles or "picket-fence-like array" described in this region of the rabbit spermatozoon by Koehler (26). He considered them as part of the "postacrosomal sheath," but the striae herein described in the guinea pig seem to us to be contained within the equatorial segment of the acrosomal cap. This interpretation is (indirectly) supported by the presence of a regular, periodic scalloping of the caudal margin of the acrosomal cap in freeze-fractured preparations of late spermatids.

Postacrosomal Plasma Membrane and Dense Lamina

The postacrosomal membrane is the major element of sperm which initially contacts the oocyte (2, 3, 49) or granulosa and other follicular cells, as well as phagocytic white blood cells (unpublished observations), before penetration or incorporation into the lysosomal system. As deter-

mined by colloidal iron hydroxide binding (45, 48), it also has a high level of acid polysaccharides. Since the first contacts between sperm and other cells frequently take place at this site, and since mucopolysaccharides are instrumental in the phenomenon of cellular "recognition," we may logically assume that the arrays in this area may serve to relay the identity of sperm to other cells.

Although this "signature" is merely general in the sense that heterologous oocytes, follicular cells, and white blood cells all interact with sperm in the same area, it may prove to be highly specific in the case of homologous oocyte-sperm recognition. It would be interesting to learn whether similar arrays are observable in the plasma membranes of oocytes and whether there are distinctive patterns in different species. Alternately, it is also probable that the patterned particles are anchoring sites for fibrils of the dense lamina beneath the membrane in this area. Indeed, *both* functions might apply.

Implantation Fossa

In the implantation fossa, the two membranes of the nuclear envelope are strictly parallel, devoid of pores, and, in one region, separated by only a few nanometers. In favorably oriented thin sections, portions of this interspace are traversed by regularly spaced linear densities about 5 nm wide and 6 nm apart (9, 38), serving to coalesce the two membranes to insure stable attachment of the articular surface of the connecting piece to the sperm head. Ventrally, the membranes of the envelope in the guinea pig are more widely separated and appear scalloped in thin section. We presume, but are not certain, that the large particles seen in freeze-fracture correspond to the region of the 15–25-nm gap rather than to the region of the narrower interspace. When the fracture plane cleaves the nuclear envelope of rat spermatozoa in this specialized region, the B face of the outer nuclear membrane shows closely packed 15-nm particles with spacing ranging to 20 nm. In the guinea pig, these particles are especially prominent and very regular in pattern. They are 20–25 nm in diameter and about 20 nm apart and do not extend over the entire area of the nuclear membrane lining the implantation fossa. In a central region over the most convex part of the articular surface of the connecting piece (the capitulum), the same membrane face may be devoid of particles. The relationship of the intramembranous particles to the linear densities observed (9, 38) traversing the narrow interspace between the two membranes in thin sections is not clear. As suggested in this paper (Fig. 18), the particles may correspond to the region where the nuclear envelope has a scalloped appearance. Here the measurements in the thin-sectioned and freeze-fractured specimens are comparable. Possibly the particles are shared by both membranes, an arrangement which would constitute a reasonable basis for partial fusion of the membranes. Alternatively, the particles may be confined to the membrane but represent sites of attachment of filaments which traverse the interspace between membranes.

Evidently, intramembranous specialization at the site of tail attachment develops quite early, for it has been observed in spermatids before nuclear condensation.

Perhaps with the exception of chloroplast lamellae (7), the nuclear envelope lying above the basal plate is apparently a unique structure, since two intracellular membranes seemingly share one large particle. The only other instance of morphological similarity is found in gap, tight, and septate junctions, which are all modifications of the plasma membrane. As suggested in the case of the gap junction particle (32), a central hollow core perpendicular to the plane of the membrane is present in the particle of the implantation fossa. But a function comparable to that of the gap junction particle in metabolic and electrotonic coupling is most unlikely, because the area surrounding the particulate array of the fossa is rich in nuclear pores. With direct communication between the nucleoplasm and cytoplasm through these pores, proposing an alternate pathway through the particle channels is unnecessary, nor is there any evidence to suggest the need for communication in a fully mature, albeit immotile, sperm.

The size of the particles (about 2 nm), their location over the basal plate, and their hollow structure strongly support their correspondence to the anchoring sites of filaments which extend from the axonemal complex to the basal plate. Since the plate is dense, it could mask these filaments in thin-sectioned material but permit visualization in freeze-fracture replicas. In fact, the distribution of particles and filaments is the same, their dimensions are similar, and both may be hollow. Architecturally, the filaments function to fasten the tail to the head and may possibly be the site of disruption and cleavage of the tail from the head by endopeptidases (34). If so, some alteration in particle distribution or structure could be sought to test this concept.

The striated ring delineating the head from the neck is arranged peripheral to the pattern of large particles and nuclear pores. Its singular structure may be due to the fact that it is the site of fusion or binding of *three* membranes, the plasma membrane and the two membranes of the nuclear envelope.

Midpiece (Mitochondrial Sheath)

The particulate strands in the plasma membrane of the guinea pig midpiece overlie the mitochondria: they occupy the same area, have a similar angulation, and are absent from interstices between mitochondria. In thin section, however, the close structural contiguity which exists between the outer mitochondrial and plasma membranes is only tenuous, and in fracture, the outer mitochondrial membrane contains no such arrays. That these particle strands represent strong physical attachments between the two membranes is questionable. More likely, the relationship is mainly functional; to determine whether it involves cation sequestration, ATP generation, or some other mitochondrial function requires far more experimentation. At any rate, the arrangement of the small particles in strands is apparently not a universal requirement for midpiece function, since it has been found only in the guinea pig so far (19, 28).

The strands do have a superficial resemblance to the flagellar necklace at the anulus of the *Lumbricus terrestris* spermatozoid (5) and to the ciliary necklace (21), but both types of "necklace" seem to fulfill the purpose of a structural attachment, and in neither do the strands overlie mitochondria. Nevertheless, their function could be that postulated by Gilula and Satir (21), i.e., participation in the control of localized membrane permeability. As in cilia, spermatozoan motility is critically dependent on the concentration of calcium, which could reasonably occur in this area.

Principal Piece

The linear array of particles opposite fiber 1 is the dominant freeze-fracture characteristic of the principal piece. Although it is more prominent in the guinea pig than in the rat and has not yet been reported in other animals except for the earthworm (5), it is a likely finding in many species. Its thin-section correlates, punctate swelling and increased density of the plasma membrane and linear fusion with the fibrous sheath, have occasionally been observed in the mouse, opossum, and human (unpublished observations).

Clearly, one function of this zipper is to attach the plasma membrane to the underlying fibrous sheath. With flagellar motility generated through the axonemal complex, the whole flagellum acquires greater efficiency in moving through points of fixation between the axonemal complex, the fibrous sheath, and the plasma membrane. Otherwise, the axonemal complex would be wavering in a relatively loose sleeve, not fully utilizing its motile power for movement of the tail (the whole tail must move for sperm to swim effectively).

Hopefully, this freeze-fracture study permitting direct visualization of structural differentiations in spermatozoan membranes will facilitate investigation of the functional specializations of these membranes and thereby enhance our understanding of this vital area of reproductive biology.

The authors acknowledge the excellent editorial assistance of Miss Rosamond Michael.

This work was supported by United States Public Health Service Grant 5 RO1 HD-06895 from the National Institute of Child Health and Human Development and Grant M 73.137 from The Population Council, New York.

Received for publication 19 February 1974, and in revised form 17 June 1974.

REFERENCES

1. AUSTIN, C. R. 1951. Observations on the penetration of the sperm into the mammalian egg. *Aust. J. Sci. Res. Ser. B.* **4**:581–597.
2. BARROS, C., and C. R. AUSTIN. 1967. In vitro fertilization and the sperm reaction in the hamster. *J. Exp. Zool.* **166**:317–324.
3. BEDFORD, J. M. 1970. Morphological aspects of sperm capacitation in mammals. *In* Advances in the Biosciences, Schering Symposium on Mechanisms Involved in Conception, Berlin, 1969. Pergamon Press GmbH, Burgplatz, W. Germany. **4**:35–50.
4. BEDFORD, J. M. 1970. Sperm capacitation and fertilization in mammals. *Biol. Reprod.* **2**(Suppl. 2):128–158.
5. BERGSTROM, B. H., and C. HENLEY. 1973. Flagellar necklaces: freeze etch observations. *J. Ultrastruct. Res.* **42**:551–553.
6. BRANTON, D., and D. W. DEAMER. 1972. Membrane structure. III. Differentiation and specialization of membranes. B. Freeze-etching. *Protoplasmatologia.* **2:E:1**:41–59.
7. BRANTON, D., and R. B. PARK. 1967. Subunits in

chloroplast lamellae. *J. Ultrastruct. Res.* **19**:283–303.

8. BURGOS, M. H., J. BLAQUIER, M. S. CAMEO, and L. GUTIERREZ. 1972. Morphological maturation of spermatozoa in the epididymis. *In* Biology of Reproduction. Symposium III, Pan American Congress of Anatomy. J. T. Vilardo and B. A. Kasprow, editors. Pan American Association of Anatomy, New Orleans, La. 367–371.
9. CHANG, M. C. 1951. Fertilizing capacity of spermatozoa deposited in the fallopian tubes. *Nature (Lond.)*. **168**:697.
10. DREVIUS, L. O. 1971. The "sperm-rise" test. *J. Reprod. Fertil.* **24**:427–429.
11. EDELMAN, G. M., and C. F. MILLETTE. 1971. Molecular probes of spermatozoan structures. *Proc. Nat. Acad. Sci. U. S. A.* **68**:2436–2440.
12. FAWCETT, D. W. 1965. The anatomy of the mammalian spermatozoon with particular reference to the guinea pig. *Z. Zellforsch. Mikrosk. Anat.* **67**:279–296.
13. FAWCETT, D. W. 1970. A comparative view of sperm ultrastructure. *Biol. Reprod.* **2**(Suppl. 2):90–127.
14. FAWCETT, D. W., and R. HOLLENBERG. 1963. Changes in the acrosome of guinea pig spermatozoa during passage through the epididymis. *Z. Zellforsch. Mikrosk. Anat.* **60**:276–292.
15. FAWCETT, D. W., and D. M. PHILLIPS. 1969. The fine structure and development of the neck region of the mammalian spermatozoon. *Anat. Rec.* **165**:153–184.
16. FAWCETT, D. W., and D. M. PHILLIPS. 1969. Observations on the release of spermatozoa and on changes in the head during passage through the epididymis. *J. Reprod. Fertil.* (Suppl. 6):405–418.
17. FLÉCHON, J. E. 1973. Influence des techniques de cryodécapage sur l'ultrastructure des spermatozoides de lapin. *J. Microsc. (Paris)*. **17**:52. a. (Abstr.).
18. FRIEND, D. S. 1973. The implantation fossa of rat sperm. *J. Ultrastruct. Res.* In press. (Abstr.).
19. FRIEND, D. S. 1973. Freeze-fracture of guinea pig sperm. *J. Ultrastruct. Res.* In press. (Abstr.).
20. FRIEND, D. S., and D. W. FAWCETT. 1973. Particle aggregates in the plasma membrane of the guinea pig sperm tail. *J. Cell Biol.* **59**(2, Pt. 2):104 a. (Abstr.).
21. GILULA, N. B., and P. SATIR. 1972. The ciliary necklace. A ciliary membrane specialization. *J. Cell Biol.* **53**:494–509.
22. GOULD, K. G. 1973. Application of in vitro fertilization. *Fed. Proc.* **32**:2069–2074.
23. GRAHAM, R. C., and M. J. KARNOVSKY. 1966. The early stages of absorption of injected horseradish peroxidase in the proximal tubules of mouse kidney. Ultrastructural cytochemistry by a new technique. *J. Histochem. Cytochem.* **14**:291–302.
24. KARNOVSKY, M. J. 1971. Use of ferrocyanide-reduced osmium tetroxide in electron microscopy. Proceedings of the 11th Annual Meeting of The American Society for Cell Biology, New Orleans, 1971. 146. (Abstr.).
25. KOEHLER, J. K. 1970. Freeze-etching studies on spermatozoa with particular reference to nuclear and postnuclear cap structure. *In* Comparative Spermatology. B. Bacetti, Editor. Academic Press, Inc., New York. 515.
26. KOEHLER, J. K. 1970. A freeze-etching study of rabbit spermatozoa with particular reference to head structures. *J. Ultrastruct. Res.* **33**:598–614.
27. KOEHLER, J. K. 1971. Human sperm head ultrastructure: a freeze-etching study. *J. Ultrastruct. Res.* **39**:520–539.
28. KOEHLER, J. K. 1973. An unusual filamentous component associated with the guinea pig sperm middle piece. *J. Microsc.* **18**:263–266.
29. KOEHLER, J. K. 1973. Studies on the postnuclear sheath of water buffalo spermatozoa. *J. Ultrastruct. Res.* **44**:355–368.
30. LEONARD, R., D. W. DEAMER, and P. ARMSTRONG. 1972. Amphibian yolk platelet ultrastructure visualized by freeze-etching. *J. Ultrastruct. Res.* **40**:1–24.
31. LUFT, J. 1971. Ruthenium red and violet. I. Chemistry, purification, methods of use for electron microscopy and mechanism of action. *Anat. Rec.* **171**:347–368.
32. MCNUTT, N. S., and R. S. WEINSTEIN. 1970.The ultrastructure of the nexus. A correlated thin section and freeze-cleave study. *J. Cell Biol.* **47**:666–688.
33. METZ, C. B. 1973. Role of specific sperm antigens in fertilization. *Fed. Proc.* **32**:2057–2064.
34. MILLETTE, C. F., P. G. SPEAR, W. E. GALL, and G. M. EDELMAN. 1973. Chemical dissection of mammalian spermatozoa. *J. Cell Biol.* **58**:662–675.
35. MIZUHIRA, V., and Y. FUTAESAKU. 1971. On the new approach of tannic acid and digitonine to the biological fixatives. Proceedings of the Electron Microscopy Society of America, 29th Annual Meeting. C. J. Arceneaux, editor. Claitor's Publishing Division, Baton Rouge, La. 494–495.
36. NICOLSON, G. L., and R. YAMAGIMACHI. 1972. Terminal saccharides on sperm plasma membranes: identification using specific agglutinins. *Science (Wash. D.C.)*. **177**:276–279.
37. PEDERSEN, H. 1972. The postacrosomal region of the spermatozoa of man and *Macaca arctoides*. *J. Ultrastruct. Res.* **40**:366–377.
38. PEDERSEN, H. 1972. Further observations on the fine structure of the human spermatozoon. *Z. Zellforsch. Mikrosk. Anat.* **123**:305–315.
39. PHILLIPS, D. M. 1972. Substructure of the mammalian acrosome. *J. Ultrastruct. Res.* **38**:591–604.
40. PLATTNER, H. 1971. Bull spermatozoa: a reinvestigation by freeze-etching using widely different cryofix-

ation procedures. *J. Submicrosc. Cytol.* **3**:19–32.

41. STAEHELIN, L. A., F. J. CHLAPOWSKI, and M. A. BONNEVILLE. 1972. Lumenal plasma membrane of the urinary bladder. I. Three-dimensional reconstruction from freeze-etch images. *J. Cell Biol.* **53**:73–91.
42. STAMBAUGH, R., and J. BUCKLEY. 1970. Subcellular localization of spermatozoal trypsin-like enzymatic activity by fluorescence microscopy. Proceedings of the Society for Reproduction, Ohio.
43. TILNEY, L. G., J. BRYAN, D. J. BUSH, K. FUJIWARA, M. S. MOOSEKER, D. B. MURPHY, and D. H. SNYDER. 1973. Microtubules: evidence for 13 protofilaments. *J. Cell Biol.* **59**:267–275.
44. WOOLEY, D. M., and D. W. FAWCETT. 1973. The degeneration and disappearance of the centrioles during the development of the rat spermatozoon. *Anat. Rec.* **177**:289–302.
45. YANAGIMACHI, R., G. L. NICOLSON, Y. D. NODA, and M. FUJIMOTO. 1973. Electron microscopic observations of the distribution of acidic anionic residues on hamster spermatozoa and eggs before and during fertilization. *J. Ultrastruct. Res.* **43**:344–353.
46. YANAGIMACHI, R., and Y. D. NODA. 1970. Ultrastructural changes in the sperm head during fertilization. *J. Ultrastruct. Res.* **31**:465–485.
47. YANAGIMACHI, R., and Y. D. NODA. 1970. Physiological changes in the postnuclear cap region of mammalian spermatozoa: a necessary preliminary to the membrane fusion between sperm and egg cells. *J. Ultrastruct. Res.* **31**:486–493.
48. YANAGIMACHI, R., Y. D. NODA, M. FUJIMOTO, and G. L. NICHOLSON. 1972. The distribution of negative surface charges on mammalian spermatozoa. *Am. J. Anat.* **135**:497–520.
49. ZAMBONI, L. 1971. Fine Morphology of Mammalian Fertilization. Harper & Row, Publishers, New York.
50. ZAMBONI, L., and M. STEFANINI. 1971. The fine structure of the neck of mammalian spermatozoa. *Anat. Rec.* **169**:155–172.